

Heat transfer characteristics of the algebraically decaying Glauert jet

Journal Article**Author(s):**

Magyari, E.; Weidman, P.D.

Publication date:

2006-12

Permanent link:

<https://doi.org/10.3929/ethz-b-000035760>

Rights / license:

[In Copyright - Non-Commercial Use Permitted](#)

Originally published in:

Heat and Mass Transfer 43(2), <https://doi.org/10.1007/s00231-006-0102-1>

E. Magyari · P. D. Weidman

Heat transfer characteristics of the algebraically decaying Glauert jet

Received: 16 June 2005 / Accepted: 25 January 2006 / Published online: 15 February 2006
© Springer-Verlag 2006

Abstract The classical *exponentially decaying* wall jet considered independently by Tetervin (NACA TN 1644 40 pp, 1948), Akatnov (Leningrad Politek Inst Trudy 5:24–31, 1953) and Glauert (J Fluid Mech 1:625–643, 1956) as well as its *algebraically decaying* counterpart (which will be referred to hereafter as “algebraic Glauert Jet”, or AG-jet for short) belong to the same similarity class of solutions of the boundary layer equations. We investigate in this paper the thermal characteristics of a nonpreheated AG-jet over a permeable wall for prescribed constant wall temperature and prescribed constant heat flux. Their scaling behavior for small and large values of the Prandtl number is discussed in detail and compared to that of the classical Tetervin–Akatnov–Glauert wall jet.

u, v Velocity components
 x, y Cartesian coordinates
 z Argument of the Airy functions (14)

Greek symbols

Γ Gamma function
 η Independent similarity variable (10)
 θ Modified similarity temperature variable (29), (30)
 κ Thermal diffusivity
 ν Kinematic viscosity
 ρ Density
 τ Shear stress (14)
 ψ Stream function

List of symbols

a, b, c Parameters (46a, b, c)
 $f(\eta)$ Similarity stream function variable (8)
 F Gauss’ hypergeometric functions (45)
 $g(\eta)$ Similarity temperature variable (9)
 k Thermal conductivity
 L Reference length
 m, n Streamwise power-law exponents (8, 9)
 Nu_x Local Nusselt number
 Pr Prandtl number
 q Heat flux
 S Dimensionless skin friction, $S=f''(0)$
 t Transformed independent variable (43)
 T Temperature
 T^* Reference temperature

Subscripts

I Prescribed constant wall temperature boundary conditions
II Prescribed constant wall heat flux boundary conditions
w Wall conditions

Superscripts

prime Derivative with respect to η

Abbreviations

AG Algebraically decaying Glauert wall jet
TAG Tetervin–Akatnov–Glauert wall jet

E. Magyari (✉)
Chair of Physics of Buildings, Institute of Building Technology,
Swiss Federal Institute of Technology (ETH) Zürich,
8093 Zurich, Switzerland
E-mail: magyari@hbt.arch.ethz.ch

P. D. Weidman
Department of Mechanical Engineering, University of Colorado,
Boulder, CO 80309-0427, USA

1 Introduction

It is well known that the classical two-dimensional free and wall jets belong to two different classes of self-similar

solutions of the boundary layer equations. In addition to these *exponentially* decaying jets, further two plane wall jet solutions belonging to the same respective similarity classes are possible, which, however, decay *algebraically* in their transversal far field. One, the algebraically decaying Airy wall jet (belonging to the similarity class of the free jet) has been considered by Weidman et al. [1] on impermeable walls, and more recently by Magyari et al. [2] on permeable walls. The existence of the second algebraically decaying wall jet (belonging to the similarity class of the classical wall jet) over a permeable wall in the presence of similarity-preserving suction, has been reported by Magyari and Keller [3]. This latter wall jet will be hereafter referred to as the “algebraic Glauert jet” or AG-jet for short.

The thermal characteristics of the Airy wall jet have been investigated by Magyari et al. [4] for prescribed constant wall temperature, by Magyari and Weidman [5] for prescribed constant wall heat flux and by Magyari and Weidman [6] for a preheated jet adjacent to an insulated wall. In [6] the thermal characteristics of the Airy jet were compared in detail with those of the classical (exponentially decaying) Tetervin [7]–Akatnov [8]–Glauert [9] wall jet (TAG-jet). The thermal characteristics of the preheated TAG-jet have been studied by Riley [10] as a part of a broader study on compressible wall jets with viscous dissipation, and also by Schwarz and Caswell [11] for the case of prescribed (constant and variable) wall temperature.

The main goal of the present paper is to investigate the thermal characteristics of the AG-jet for constant temperature and constant wall heat flux conditions at the permeable wall. The scaling behavior of the thermal characteristics for small and large Prandtl number will also be discussed in detail and compared to that of the classical TAG-jet.

2 Governing equations

We consider a planar wall jet issuing in a host fluid through a narrow slot. The jet is not preheated, i.e., its entrance temperature coincides with the ambient temperature T_∞ of the host fluid. The wall is permeable and a similarity-preserving suction is applied. The z -axis is parallel to the slot, and x and y are the streamwise and wall normal Cartesian coordinates, respectively. As usual (see, e.g., Schlichting and Gersten [12]), the coordinate x is measured from a virtual origin behind the slot. As shown recently by Revuelta et al. [13], the concept of the virtual origin serves not only to avoid the singular behavior of the self-similar jet solutions, but it even represents a first order correction to their leading order far field description.

For incompressible flow in the boundary layer approximation, neglecting buoyancy and viscous self-heating effects, the dimensional equations governing conservation of mass, momentum and energy are

$$u_x + v_y = 0, \quad (1)$$

$$uu_x + vv_y = \nu u_{yy}, \quad (2)$$

$$uT_x + vT_y = \kappa T_{yy}, \quad (3)$$

where ν and κ are the momentum and thermal diffusivities, respectively, and subscripts denote partial derivatives with respect to a coordinate.

The flow and thermal boundary conditions of interest in this study are:

I. Prescribed constant wall temperature:

$$u = 0 \quad (y = 0), \quad (4a)$$

$$v = v_w(x) \quad (y = 0), \quad (4b)$$

$$T = \text{const} \equiv T_w > T_\infty \quad (y = 0), \quad (4c)$$

$$u \rightarrow 0 \quad (y \rightarrow \infty), \quad (4d)$$

$$T \rightarrow T_\infty \quad (y \rightarrow \infty). \quad (4e)$$

II. Prescribed constant wall heat flux:

$$u = 0 \quad (y = 0), \quad (5a)$$

$$v = v_w(x) \quad (y = 0), \quad (5b)$$

$$q = \text{const} \equiv q_w \quad (y = 0), \quad (5c)$$

$$u \rightarrow 0 \quad (y \rightarrow \infty), \quad (5d)$$

$$T \rightarrow T_\infty \quad (y \rightarrow \infty), \quad (5e)$$

where $v = v_w(x)$ is the velocity of a lateral suction of the fluid.

3 Similarity formulation

We introduce the stream function $(u, v) = (\psi_y, -\psi_x)$ and write the governing equations as

$$\psi_y \psi_{xy} - \psi_x \psi_{yy} = \nu \psi_{yyy}, \quad (6)$$

$$\psi_y T_x - \psi_x T_y = \kappa T_{yy}. \quad (7)$$

A suitable general power-law similarity *ansatz* is given by:

$$\psi(x, y) = \frac{2\nu}{m+1} \left(\frac{x}{L}\right)^{(m+1)/2} f(\eta), \quad (8)$$

$$T(x, y) = T_\infty + T_* \left(\frac{x}{L}\right)^n g(\eta), \quad (9)$$

$$\eta = \left(\frac{x}{L}\right)^{(m-1)/2} \frac{y}{L}, \quad (10)$$

where L is a reference length, T_* a reference temperature and $m \neq -1$. The dimensional velocity components are then

$$u(x, y) = \frac{2}{m+1} \frac{\nu}{L} \left(\frac{x}{L}\right)^m f'(\eta), \quad (11)$$

$$v(x, y) = -\frac{\nu}{L} \left(\frac{x}{L}\right)^{(m-1)/2} \left[f(\eta) + \frac{m-1}{m+1} \eta f'(\eta) \right]. \quad (12)$$

The dimensional suction velocity is given by

$$v_w(x) = -\frac{\nu}{L} \left(\frac{x}{L}\right)^{(m-1)/2} f(0), \quad (13)$$

the skin friction by

$$\tau_w(x) = -\frac{\rho v^2}{L^2} \frac{2}{m+1} \left(\frac{x}{L}\right)^{(3m-1)/2} f''(0), \quad (14)$$

the wall temperature distribution by

$$T_w(x) = T_\infty + T_* \left(\frac{x}{L}\right)^n g(0) \quad (15)$$

and the wall heat flux by

$$q_w(x) = -\frac{kT_*}{L} \left(\frac{x}{L}\right)^{(2n+m-1)/2} g'(0). \quad (16)$$

The equations satisfied by the similarity functions $f(\eta)$ and $g(\eta)$ are

$$f''' + ff'' - \frac{2m}{m+1} f'^2 = 0, \quad (17)$$

$$\frac{1}{Pr} g'' + fg' - \frac{2n}{m+1} f'g = 0, \quad (18)$$

where a prime denotes differentiation with respect to η and $Pr = \nu / \kappa$ is the Prandtl number.

The flow boundary value problem is decoupled from the thermal problems. The corresponding boundary conditions for cases I and II are identical, namely

$$f(0) = f_w, \quad (19a)$$

$$f'(0) = 0, \quad (19b)$$

$$f'(\eta) \rightarrow 0 \quad \text{as } \eta \rightarrow \infty, \quad (19c)$$

where f_w denotes the (positive) suction parameter.

Two “nonlinear eigenvalues” m of the flow boundary value problem (17) and (19a, b, c) are known. These values $m = -1/3$ and $m = -1/2$, governing the streamwise scale of the self-similar flows are associated with two differential invariants of (1), (2) and (4a, b) specifying two different similarity cases of jets. To $m = -1/3$ there corresponds the classical (exponentially decaying) Schlichting–Bickley free jet [14, 15] as well as the algebraically decaying Airy wall jet [1, 2], while to $m = -1/2$ there corresponds the classical (exponentially decaying) TAG-jet [7–9] as well as its algebraically decaying counterpart the AG-jet [3]. The role of the nonlinear eigenvalues becomes apparent by observing that (17) may be written in the two distinct forms

$$f^{-1} \frac{d}{d\eta} \left[f^{3/2} \frac{d}{d\eta} \left(f^{-1/2} f' + \frac{2}{3} f^{3/2} \right) \right] - \frac{2(2m+1)}{m+1} f'^2 = 0 \quad (20)$$

and

$$\frac{d^2}{d\eta^2} \left(f' + \frac{1}{2} f^2 \right) - \frac{3m+1}{m+1} f'^2 = 0 \quad (21)$$

showing that the last term in (20) vanishes when $m = -1/2$ and the last term in (21) vanishes when $m = -1/3$. As pointed out recently by Krechetnikov and Lipatov [16] these two nonlinear eigenvalues are singled out in fact by a symmetry property, by some “hidden invariances” of the basic equations and not by an asymptotic

requirement concerning the way in which the transversal far field of the corresponding decays.

The present investigation is concerned only with the AG- and TAG-jets corresponding to the nonlinear eigenvalue $m = -1/2$. However, for the sake of transparency, in Table 1 the nomenclature, the asymptotic behavior and the main references have been collected for all the four types of laminar jets associated with the nonlinear eigenvalues $m = -1/2$ and $m = -1/3$.

4 The AG-jet solution

For $m = -1/2$ (20) yields the first integral

$$f^{3/2} \frac{d}{d\eta} \left(f^{-1/2} f' + \frac{2}{3} f^{3/2} \right) = \text{const.} \quad (22)$$

Evaluation of this equation $\eta=0$ and taking into account the boundary conditions (19a, b, c) one obtains for the integration constant the value $f_w S$ where $S \equiv f''(0)$ is the dimensionless skin friction. Thus, (22) becomes

$$2ff'' + 2f^2 f' - f'^2 = 2Sf_w. \quad (23)$$

For an impermeable wall ($f_w = 0$) one recovers in (23) the equation of the TAG-jet. With suction ($f_w \neq 0$), however, a wall jet solution with algebraic asymptotic decay

$$f'(\eta) \rightarrow \gamma \eta^{-2/3}, \quad (24a)$$

i.e.,

$$f(\eta) \rightarrow 3\gamma \eta^{1/3} \quad \text{as } \eta \rightarrow \infty \quad (24b)$$

emerges for positive constant γ , [3]. Evaluation of (23) as $\eta \rightarrow \infty$, using the behaviors given in (24a, b), immediately furnishes the scale factor γ of the asymptotic decay of the jet velocity

$$\gamma = \left(\frac{Sf_w}{9} \right)^{1/3}. \quad (25)$$

Table 1 Overview of the laminar jets associated with the nonlinear eigenvalues $m = -1/2$ and $m = -1/3$

Nonlinear eigenvalue m	Asymptotic decay		References
	Exponential	Algebraic	
-1/2	Tetervin–Akatnov–Glauert wall Jet (TAG-jet)		[7–13, 16]
		Algebraic Glauert wall jet (AG-jet)	[3, present]
-1/3	Schlichting–Bickley free jet		[12–16]
		Airy wall jet	[1, 2, 4–6]

Since the skin friction parameter S is positive [3], f_w must also be positive. This requires according to (13) the following distribution of the (dimensional) suction velocity along the wall

$$v_w(x) = -\frac{v}{L} \left(\frac{x}{L}\right)^{-3/4} f_w. \quad (26)$$

For any specified value of $f_w > 0$ there exists a family of AG-jet solutions depending on the parameter S . For $S = 2/9$, corresponding to the TAG-jet normalization used by Glauert [9], we have from (25) $\gamma = (2f_w/81)^{1/3}$ and the AG-jet corresponding to a specified value of f_w is obtained as the unique solution of the initial value problem

$$2ff'' + 2f^2f' - f'^2 = 4f_w/9, \quad (27a)$$

$$f(0) = f_w, \quad (27b)$$

$$f'(0) = 0. \quad (27c)$$

It is worth underlining here that the AG-jet emerges from the same balance equations and boundary conditions as the classical TAG-jet. The approach leading to the AG-jet is also exactly the same, except that it relaxes two of Glauert's initial restrictions, namely:

1. The explicit restriction to an impermeable wall, and
2. The tacit restriction to an exponential decay (more precisely to a decay which is faster than $\eta^{-2/3}$).

As previously shown in [3], the AG-jet solution (27a, b, c) tends precisely to the TAG-jet as $f_w \rightarrow 0$. This gradual crossover of the AG-jet into the TAG-jet is illustrated in Fig. 1. In the sequel, only AG-jets with skin friction parameter $S = 2/9$ will be considered.

5 Associated thermal boundary value problems

The thermal boundary value problems I and II are coupled to the flow problem (27a, b, c) as follows.

I. Prescribed constant wall temperature:

According to (15), the temperature exponent $n = 0$ is required. Thus, the thermal boundary value problem is

$$\frac{1}{Pr} g'' + fg' = 0, \quad (28a)$$

$$g(0) = +1, \quad (28b)$$

$$g(\infty) = 0. \quad (28c)$$

The temperature field is given by $T = T_\infty + T_* g(\eta)$, where the reference temperature T_* is specified by the prescribed value T_w of the wall temperature. In this way, $T_* = T_w - T_\infty$ and

$$T = T_\infty + (T_w - T_\infty)g(\eta). \quad (29)$$

The quantity of primary engineering interest is the wall heat flux distribution which, according to (16), becomes in this case

$$q_w(x) = -\frac{k(T_w - T_\infty)}{L} \left(\frac{x}{L}\right)^{-3/4} g'(0). \quad (30)$$

The corresponding local Nusselt number $Nu_x = (q_w x/k)/(T_w - T_\infty)$ leads in this case to the average Nusselt number

$$\langle Nu_x \rangle_I = \frac{1}{L} \int_0^L Nu_x dx = -\frac{4}{5} g'(0). \quad (31)$$

II. Prescribed constant wall heat flux:

According to (15) the temperature exponent required for constant wall heat flux is $n = (1 - m)/2 = 3/4$. Thus, the corresponding thermal boundary value problem is

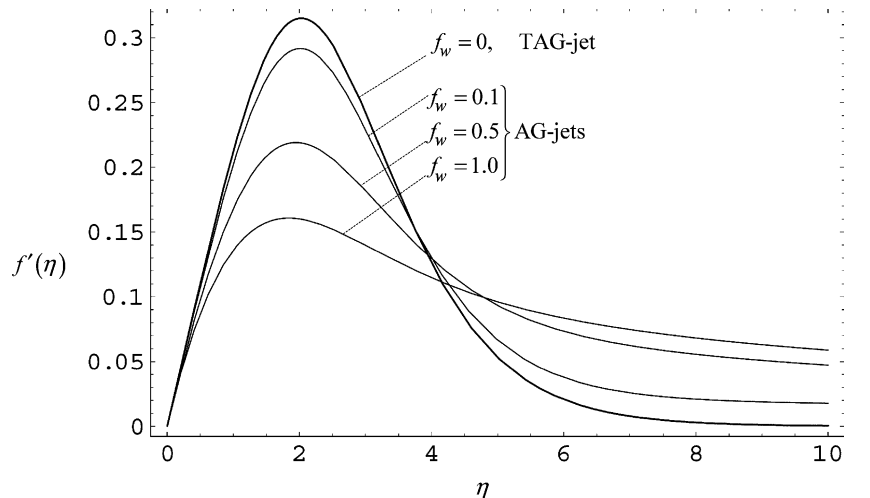
$$\frac{1}{Pr} g'' + fg' - 3f'g = 0, \quad (32a)$$

$$g'(0) = -1, \quad (32b)$$

$$g(\infty) = 0. \quad (32c)$$

The temperature field is given by $T = T_\infty + T_*(x/L)^{3/4} g(\eta)$ where the reference temperature T_* is

Fig. 1 Gradual crossover of the AG-jet into the TAG-jet as $f_w \rightarrow 0$



specified by the prescribed value of the wall heat flux, $q_w = kT_* / L$. In this way one obtains

$$T = T_\infty + \frac{q_w L}{k} \left(\frac{x}{L}\right)^{3/4} g(\eta), \quad (33)$$

and hence the wall temperature distribution is

$$T_w = T_\infty + \frac{q_w L}{k} \left(\frac{x}{L}\right)^{3/4} g(0). \quad (34)$$

The local Nusselt number $Nu_x = (q_w x / k) / (T_w - T_\infty)$ leads in this case to the average Nusselt number

$$\langle Nu_x \rangle_{II} = \frac{1}{L} \int_0^L Nu_x dx = \frac{4}{5} \frac{1}{g(0)}. \quad (35)$$

6 Dependence on f_w and Pr

We investigate in this section the dependence on f_w and Pr of the average Nusselt numbers governed by $g'(0)$ for constant prescribed wall temperature and $g(0)$ for constant prescribed wall heat flux, for both the TAG- and the AG-jets.

I. Prescribed constant wall temperature:

The corresponding boundary value problem (28a, b, c) has been solved for the TAG-jet several decades ago by Riley [10] as a part of a broader study of compressible wall jets with viscous dissipation (see also Schwarz and Caswell [11]). The dimensionless wall temperature gradient $g'(0)$ is readily obtained in this case with the aid of the first integral of (23) for $f_w = 0$, namely

$$f' = \frac{2}{3} (f^{1/2} - f^2) \quad (\text{TAG-jet}), \quad (36)$$

(28a, b, c) and (36) then yield

$$g'(\eta) = g'(0) \exp \left(-Pr \int_0^\eta f d\eta \right) = g'(0) (1 - f^{3/2})^{Pr}. \quad (37)$$

Furthermore,

$$\begin{aligned} g(\eta) &= 1 + g'(0) \int_0^\eta (1 - f^{3/2})^{Pr} d\eta \\ &= 1 + \frac{3}{2} g'(0) \int_0^f f^{-1/2} (1 - f^{3/2})^{Pr-1} df. \end{aligned} \quad (38)$$

Letting here $\eta \rightarrow \infty$ and taking into account $f(\infty) = 1$, we recover the known result [10, 11]

$$g'(0) = -\frac{\Gamma(Pr + 1/3)}{\Gamma(1/3)\Gamma(Pr)} \quad (\text{TAG-jet}) \quad (39)$$

and, therefore, according to (31),

$$\langle Nu_x \rangle_I = \frac{4}{5} \frac{\Gamma(Pr + 1/3)}{\Gamma(1/3)\Gamma(Pr)} \quad (\text{TAG-jet}). \quad (40)$$

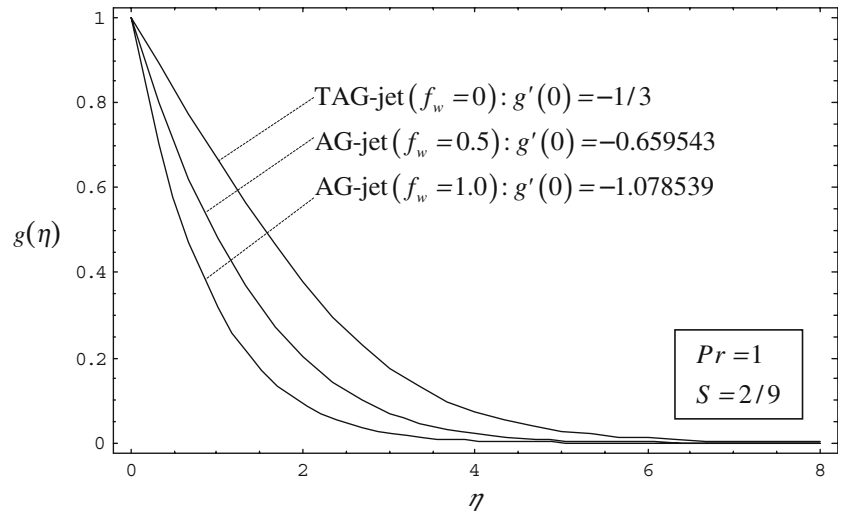
For the AG-jet, although the first part of (37) holds also in this case, only numerical solutions are possible. As a first illustration in Fig. 2 the dimensionless temperature profiles $g(\eta)$ are plotted for both the TAG- and the AG-jets at $Pr = 1$, in the latter case for suction parameter values $f_w = 0.5$ and 1.

We now turn our attention to the Prandtl number dependence of $g'(0)$. Taking into account the properties of the Gamma function [17], we deduce from (33) the following scaling behavior for the TAG-jet

$$-g'(0) \rightarrow Pr \quad \text{for } Pr \rightarrow 0, \quad (41a)$$

$$-g'(0) \rightarrow \frac{\sum_{j=0}^{\infty} (1/3^j j!)}{\Gamma(1/3) \exp(1/3)} Pr^{1/3} = 0.373282 Pr^{1/3} \quad \text{for } Pr \rightarrow \infty, \quad (41b)$$

Fig. 2 Dimensionless similar temperature profiles for the TAG- and AG-jet, respectively, for a prescribed constant wall temperature



and thus the asymptotic forms of the average Nusselt number (40) are given by

$$\langle Nu_x \rangle_I = \begin{cases} 0.8Pr & \text{for } Pr \rightarrow 0 \\ 0.298626Pr^{1/3} & \text{for } Pr \rightarrow \infty \end{cases} \quad (\text{TAG-jet}). \quad (41c)$$

The full dependence on Pr of the average Nusselt number (40) of the TAG-jet in the range $0 < Pr \leq 10$ is shown in Fig. 3.

For the AG-jet, numerical solution of the boundary value problem (27a, b, c) for $f_w = 1$ yields

$$-g'(0) = \begin{cases} 0.793663Pr^{3/4} & \text{for } Pr \rightarrow 0 \\ Pr & \text{for } Pr \rightarrow \infty \end{cases} \quad (42a) \\ (\text{AG-jet}, f_w = 1),$$

and thus

$$\langle Nu_x \rangle_I = \begin{cases} 0.634930Pr^{3/4} & \text{for } Pr \rightarrow 0 \\ 0.8Pr & \text{for } Pr \rightarrow \infty \end{cases} \quad (42b) \\ (\text{AG-jet}, f_w = 1).$$

Comparison of (41c) with (42b) shows that the average Nusselt numbers of the TAG- and AG-jets scale differently with Pr in both the small and large Prandtl number limits.

II. Prescribed constant wall heat flux:

The quantity of primary physical interest here according to (35) is the dimensionless wall temperature $g(0)$, determined from the solution of the boundary value problem (32a, b, c). For the TAG-jet the result can be obtained analytically again as follows.

Following Riley [10], the variable transformation $t = 1 - f^{3/2}$ (43)

is introduced to rewrite the boundary value problem (32a, b, c) as

$$t(1-t)\frac{d^2g}{dt^2} + \left[1 - Pr - \left(\frac{5}{3} - Pr\right)t\right]\frac{dg}{dt} - 2Prg = 0, \quad (44a)$$

$$\lim_{t \rightarrow 1} \left[t(1-t)^{2/3} \frac{dg}{dt} \right] = 1, \quad (44b)$$

$$g|_{t=0} = 0. \quad (44c)$$

The general solution of (44a) is a linear combination of the hypergeometric functions [17]. Given here in the form

$$g = AF(a, b; a + b + 1 - c; 1 - t) + B(1 - t)^{1/3}F(c - b, c - a; c - a - b + 1; 1 - t), \quad (45)$$

where A and B are constants and

$$c = 1 - Pr, \quad (46a)$$

$$a = \frac{1}{6} \left(2 - 3Pr + \sqrt{9Pr^2 - 84Pr + 4} \right), \quad (46b)$$

$$b = \frac{1}{6} \left(2 - 3Pr - \sqrt{9Pr^2 - 84Pr + 4} \right). \quad (46c)$$

Using the properties of the hypergeometric functions [17], the boundary conditions (44a, b, c) determine the constants in

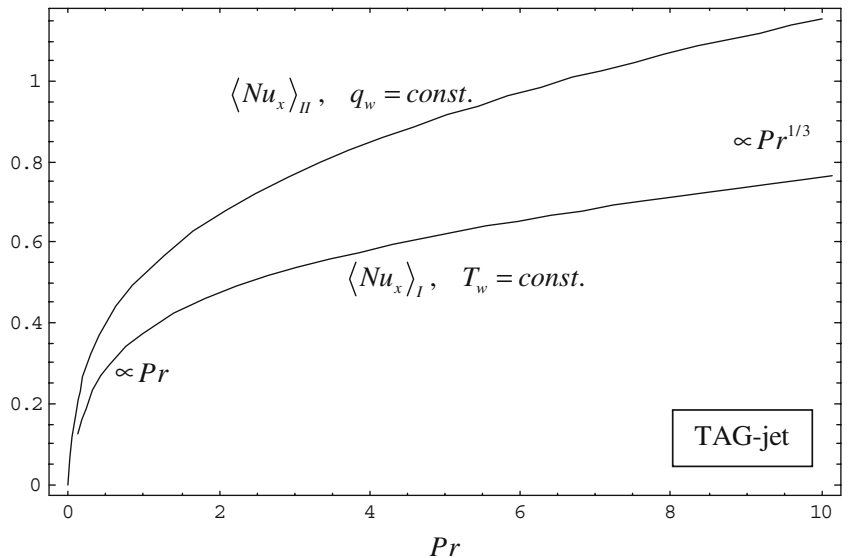
$$A = 3 \frac{F(c - b, c - a; 4/3; 1)}{F(a, b; 2/3; 1)}, \quad B = -3 \quad (47)$$

in (45). In this way, we obtain for the reciprocal value of the dimensionless wall temperature

$$\frac{1}{g(0)} = \frac{1}{3} \frac{F(a, b; 2/3; 1)}{F(c - b, c - a; 4/3; 1)} \quad (48)$$

Further use hypergeometric functions properties shows that (48) can be transformed into

Fig. 3 Plot of the average Nusselt numbers (40) and (50) of the TAG-jet as a function of Pr for prescribed constant wall temperature and constant wall heat flux, respectively



$$\frac{1}{g(0)} = \frac{\Gamma(2/3)}{\Gamma(1/3)} \frac{\Gamma(1/3 + Pr + a)\Gamma(1/3 + Pr + b)}{\Gamma(2/3 - a)\Gamma(2/3 - b)} \quad (49)$$

(TAG-jet),

and thus, according to (35)

$$\langle Nu_x \rangle_{II} = \frac{4\Gamma(2/3)}{5\Gamma(1/3)} \frac{\Gamma(1/3 + Pr + a)\Gamma(1/3 + Pr + b)}{\Gamma(2/3 - a)\Gamma(2/3 - b)} \quad (50)$$

(TAG-jet).

The AG-jet solutions again are only available through numerical solution of boundary value problem (32a, b, c). As an illustration in Fig. 4, dimensionless temperature profiles $g(\eta)$ are plotted for $Pr = 1$, both for the TAG- and AG-jets, in the latter case for the values $f_w = 0.5$ and 1 of the suction parameter.

The Prandtl number dependence of $g(0)$ may be determined as follows.

Taking into account the properties of the Gamma function [17], we deduce from (49) the following scaling behavior (for the TAG-jet)

$$\frac{1}{g(0)} \rightarrow 4Pr \quad \text{for } Pr \rightarrow 0, \quad (51a)$$

$$\frac{1}{g(0)} \rightarrow \frac{9}{5\Gamma(1/3)} Pr^{1/3} \quad \text{for } Pr \rightarrow \infty, \quad (51b)$$

and hence

$$\frac{1}{g(0)} = \begin{cases} 4Pr & \text{for } Pr \rightarrow 0 \\ 0.671908Pr^{1/3} & \text{for } Pr \rightarrow \infty \end{cases} \quad \text{(TAG-jet).} \quad (51c)$$

Thus, the corresponding average Nusselt number given in (35) becomes

$$\langle Nu_x \rangle_{II} = \begin{cases} 3.2Pr & \text{for } Pr \rightarrow 0 \\ 0.537526Pr^{1/3} & \text{for } Pr \rightarrow \infty \end{cases} \quad \text{(TAG-jet).} \quad (52)$$

The full dependence on Pr of the average Nusselt number (50) of the TAG-jet in the range $0 < Pr \leq 10$ is shown also in Fig. 3.

For the AG-jet numerical solution of the boundary value problem (27a, b, c) for $f_w = 1$ yields

$$\frac{1}{g(0)} = \begin{cases} 2.473968Pr^{3/4} & \text{for } Pr \rightarrow 0 \\ Pr & \text{for } Pr \rightarrow \infty \end{cases} \quad \text{(AG-jet, } f_w = 1), \quad (53a)$$

and thus

$$\langle Nu_x \rangle_{II} = \begin{cases} 1.979174Pr^{3/4} & \text{for } Pr \rightarrow 0 \\ 0.8Pr & \text{for } Pr \rightarrow \infty \end{cases} \quad \text{(AG-jet, } f_w = 1). \quad (53b)$$

Comparing (53b) with (52) one immediately sees that the average Nusselt numbers of the TAG- and AG-jets scale with the Prandtl number also in this case quite differently. The full dependence on Pr of the average Nusselt numbers (42b) and (53b) of the AG-jet in the ranges $Pr \leq 10^{-3}$ and $0 < Pr \leq 10$ is shown in Figs. 5 and 6, respectively.

7 Summary and conclusions

The scaling behavior of the average Nusselt numbers of the TAG and AG wall jets for small and large values of the Prandtl number Pr are summarized for prescribed constant wall temperature T_w (subscript I) and for constant wall heat flux q_w (subscript II) in Table 2. The full dependence on Pr of these quantities in extended ranges Pr is shown in Figs. 3, 5 and 6.

Table 2 shows that the Nusselt numbers $\langle Nu_x \rangle_I$ and $\langle Nu_x \rangle_{II}$ of the TAG- and AG-jets scale for small values of Pr with Pr and $Pr^{3/4}$, respectively, while for large values of Pr they scale with $Pr^{1/3}$ and Pr , respectively.

It is therefore concluded that the TAG- and AG-jets, although they belong to the same similarity class, can be

Fig. 4 Dimensionless similar temperature profiles for the TAG- and AG-jet, respectively, for a prescribed constant wall heat flux

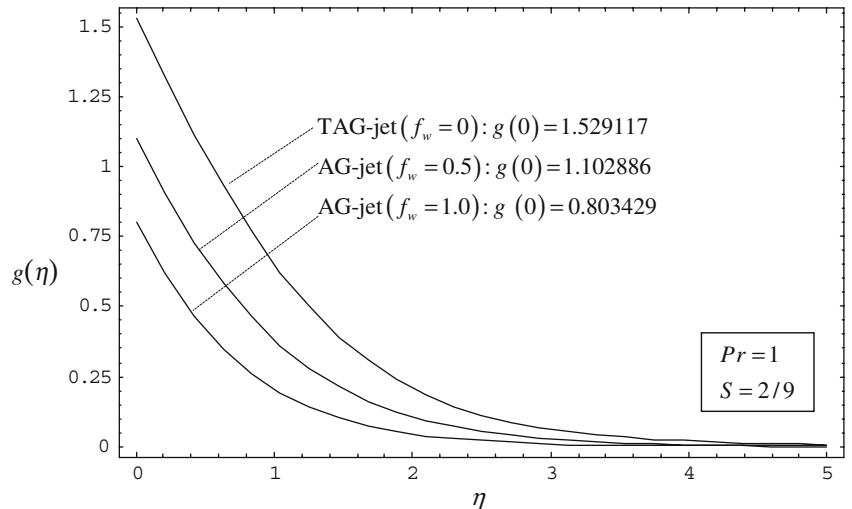


Fig. 5 Plot of the average Nusselt numbers of the AG-jet as a function of Pr for prescribed constant wall temperature and constant wall heat flux, respectively, in the range $Pr \leq 10^{-3}$ where they both scale according to (53b) with $Pr^{3/4}$ (as $Pr \rightarrow 0$)

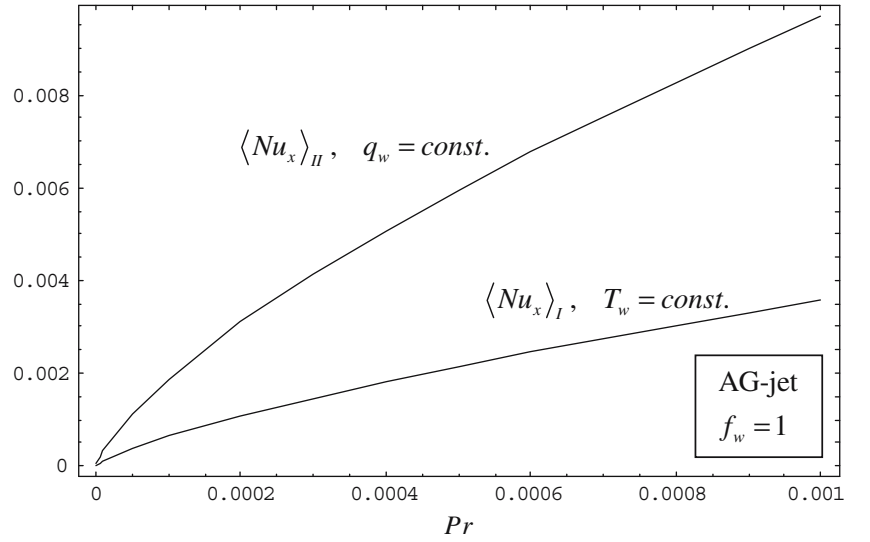


Fig. 6 Plot of the average Nusselt numbers of the AG-jet as a function of Pr for prescribed constant wall temperature and constant wall heat flux, respectively, in the range $1 \leq Pr \leq 10$ where they both scale according to (53b) with Pr (as $Pr \rightarrow \infty$). For $Pr=10$, $\langle Nu_x \rangle_I$ exceeds the asymptotic value $0.8Pr=8$ only by 0.2% and $\langle Nu_x \rangle_{II}$ by 0.8%

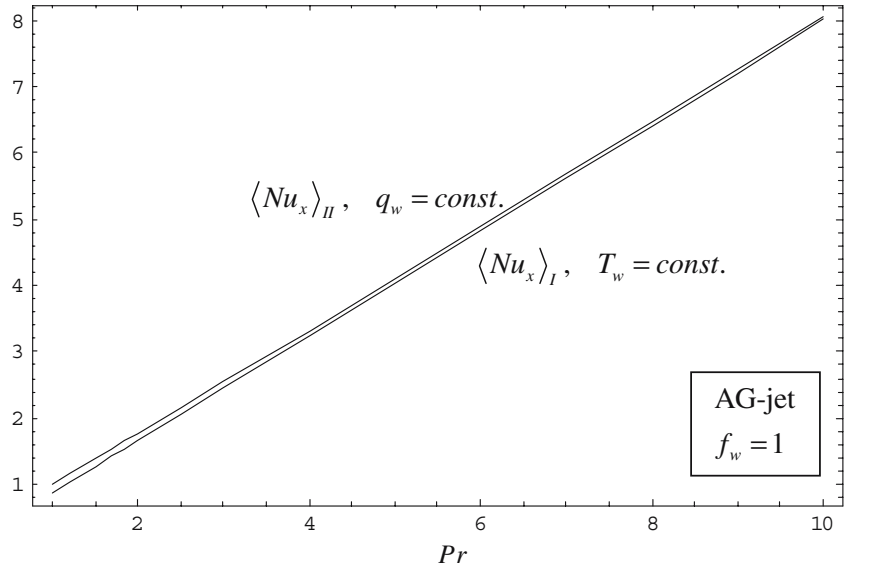


Table 2 Overview of the Prandtl number dependence of the average Nusselt numbers of the TAG- and AG-jets, respectively

Average Nusselt number	Jet	$Pr \rightarrow 0$	$Pr \rightarrow \infty$
$\langle Nu_x \rangle_I = \frac{4}{5}[-g'(0)] = (T_w = \text{const})$	TAG-jet	$0.8Pr$ (41c)	$0.298626 Pr^{1/3}$ (41c)
	AG-jet ($f_w = 1$)	$0.634930 Pr^{3/4}$ (42b)	$0.8Pr$ (42b)
$\langle Nu_x \rangle_{II} = \frac{4}{5} \frac{1}{g(0)} = (q_w = \text{const})$	TAG-jet	$3.2Pr$ (52)	$0.537526 Pr^{1/3}$ (52)
	AG-jet ($f_w = 1$)	$1.979174 Pr^{3/4}$ (53b)	$0.8Pr$ (53b)

distinguished from each other not only by their far field behavior (exponential vs. algebraic decay) but also by the Prandtl number-dependence of their main thermal characteristics (see Tables 1 and 2).

References

1. Weidman PD, Kubitschek DG, Brown SN (1997) Boundary layer similarity flow driven by power-law shear. *Acta Mech* 120:199–215
2. Magyari E, Keller B, Pop I (2003) Boundary layer similarity flow driven by a power-law shear over a permeable plane surface. *Acta Mech* 163:139–146
3. Magyari E, Keller B (2004) The algebraically decaying wall jet. *Eur J Mech B: Fluids* 23:601–605
4. Magyari E, Keller B, Pop I (2004) Heat transfer characteristics of a boundary layer flow driven by a power-law shear over a semi-infinite flat plate. *Int J Heat Mass Transf* 47:31–34
5. Magyari E, Weidman PD (2004) Thermal characteristics of the Airy wall jet for constant surface heat flux. *Heat Mass Transf* (Published online, 1 Dec 2005)
6. Magyari E, Weidman PD (2005) The preheated Airy wall jet. *Heat Mass Transf* 41:1014–1020
7. Tetervin N (1948) Laminar flow of a slightly viscous incompressible fluid that issues from a slit and passes over a flat plate. NACA TN 1644. Washington, DC, 40 pp
8. Akatnov NI (1953) Development of 2D laminar jet along a solid surface. *Leningr Politek Inst Trudy* 5:24–31
9. Glauert MB (1956) The wall jet. *J Fluid Mech* 1:625–643
10. Riley N (1958) Effects of compressibility on a laminar wall jet. *J Fluid Mech* 4:615–628
11. Schwarz WH, Caswell B (1961) Some heat transfer characteristics of the two dimensional laminar incompressible wall jet. *Chem Eng Sci* 16:338–351
12. Schlichting H, Gersten K (2000) *Boundary layer theory*. Springer, Berlin Heidelberg New York
13. Revuelta A, Sanchez AL, Linan A (2002) The virtual origin as a first order correction for the far-field description of laminar jets. *Phys Fluids* 14:1821–1824
14. Schlichting H (1933) Laminare strahlausbreitung. *J Appl Math Mech (ZAMM)* 13:260–263
15. Bickley WG (1937) The plane jet. *Phil Mag* 23:727–730
16. Krechetnikov R, Lipatov I (2002) Hidden invariances in problems of two dimensional and three dimensional wall jets for Newtonian and non-Newtonian fluids. *SIAM J Appl Math* 62:1837–1855
17. Abramowitz M, Stegun IA (1972) *Handbook of mathematical functions*. US Government Printing Office, Washington, DC